



# Large-Eddy/Lattice Boltzmann Simulations of Micro-Blowing Strategies for Subsonic and Supersonic Drag Control

Suresh Menon  
Georgia Institute of Technology, Atlanta, Georgia

## The NASA STI Program Office . . . in Profile

Since its founding, NASA has been dedicated to the advancement of aeronautics and space science. The NASA Scientific and Technical Information (STI) Program Office plays a key part in helping NASA maintain this important role.

The NASA STI Program Office is operated by Langley Research Center, the Lead Center for NASA's scientific and technical information. The NASA STI Program Office provides access to the NASA STI Database, the largest collection of aeronautical and space science STI in the world. The Program Office is also NASA's institutional mechanism for disseminating the results of its research and development activities. These results are published by NASA in the NASA STI Report Series, which includes the following report types:

- **TECHNICAL PUBLICATION.** Reports of completed research or a major significant phase of research that present the results of NASA programs and include extensive data or theoretical analysis. Includes compilations of significant scientific and technical data and information deemed to be of continuing reference value. NASA's counterpart of peer-reviewed formal professional papers but has less stringent limitations on manuscript length and extent of graphic presentations.
- **TECHNICAL MEMORANDUM.** Scientific and technical findings that are preliminary or of specialized interest, e.g., quick release reports, working papers, and bibliographies that contain minimal annotation. Does not contain extensive analysis.
- **CONTRACTOR REPORT.** Scientific and technical findings by NASA-sponsored contractors and grantees.

- **CONFERENCE PUBLICATION.** Collected papers from scientific and technical conferences, symposia, seminars, or other meetings sponsored or cosponsored by NASA.
- **SPECIAL PUBLICATION.** Scientific, technical, or historical information from NASA programs, projects, and missions, often concerned with subjects having substantial public interest.
- **TECHNICAL TRANSLATION.** English-language translations of foreign scientific and technical material pertinent to NASA's mission.

Specialized services that complement the STI Program Office's diverse offerings include creating custom thesauri, building customized databases, organizing and publishing research results . . . even providing videos.

For more information about the NASA STI Program Office, see the following:

- Access the NASA STI Program Home Page at <http://www.sti.nasa.gov>
- E-mail your question via the Internet to [help@sti.nasa.gov](mailto:help@sti.nasa.gov)
- Fax your question to the NASA Access Help Desk at 301-621-0134
- Telephone the NASA Access Help Desk at 301-621-0390
- Write to:  
NASA Access Help Desk  
NASA Center for Aerospace Information  
7121 Standard Drive  
Hanover, MD 21076



# Large-Eddy/Lattice Boltzmann Simulations of Micro-Blowing Strategies for Subsonic and Supersonic Drag Control

Suresh Menon  
Georgia Institute of Technology, Atlanta, Georgia

Prepared under Grant NAG3-2653

National Aeronautics and  
Space Administration

Glenn Research Center

The Propulsion and Power Program at  
NASA Glenn Research Center sponsored this work.

Available from

NASA Center for Aerospace Information  
7121 Standard Drive  
Hanover, MD 21076

National Technical Information Service  
5285 Port Royal Road  
Springfield, VA 22100

Available electronically at <http://gltrs.grc.nasa.gov>

# Large-Eddy/Lattice Boltzmann Simulations of Micro-Blowing/Suction Strategies For Subsonic and Supersonic Drag Control

Suresh Menon  
Georgia Institute of Technology  
Atlanta, Georgia 30332

## 1. Introduction

In recent years, a novel drag reduction method in turbulent boundary layers has been demonstrated using a micro-blowing technique (MBT) at NASA GRC (Hwang [1], Hwang and Biesiaday [2]; Hwang, 1998 [3], Tillman and Hwang, 1999 [4], Welch et al., [5]). Key features of this technique (in contrast to earlier more conventional blowing method) are the low effective roughness for the porous skin (achieved due to the use of micro holes) and the minimal amount of injection flow rate needed to achieve drag control. Results under laboratory and full-scale operating conditions show that large skin friction drag reduction (as much as 50 to 70 percent) can be achieved using MBT. Application of MBT to turbulent supersonic boundary layers has also shown that even higher drag reduction can be achieved. Furthermore, a reduction of noise was also observed in the supersonic case. Interesting observations in subsonic flow are that drag can be controlled by adjusting the injection flow rate and that the maximum drag reduction appears to occur within regions of adverse pressure gradient. However, more recent results in strongly adverse pressure gradient flow on a strut suggest that micro-blowing can lead to increased boundary layer and wake thickness [5] which can result in an increase in pressure drag for external flows. Thus, there are still many unresolved questions regarding the underlying physics of drag reduction as achieved by the MBT and how this blowing process impacts the larger-scale flow features. Furthermore, the experimental data suggests that the injection system (and the injected airflow) couple strongly with the outer (primary) flow especially in adverse pressure gradient flow. This makes the optimization of the design of this device problematic and parametric study using primarily an experimental approach is not a cost-effective approach.

Numerical studies of the MBT in subsonic turbulent boundary layers have also been recently reported [6] in which a steady-state 3D code was used. Both the micro holes and the cross-stream boundary layer were numerically modeled using a low Reynolds number turbulence closure. Results showed that for all the simulated cases, micro-blowing can potentially lead to unsteadiness due to the formation of vortices. However, due to the steady-state model employed this feature could not be studied. A recent study (Menon [7]; Cammarato and Menon [8]) studied Micro-Electro-Mechanical System (MEMS) based micro-scale blowing/suction devices in a supersonic boundary layer using direct numerical simulation (DNS). Significant unsteadiness is shown to be associated with the interaction between the injected fluid and the supersonic boundary layer. Vortex shedding and even pairing occurs in the near field of the injected fluid in the boundary layer. By combining blowing and suction it was further shown that not only drag can be reduced but also that it can be increased at specific location.

It is clear that DNS of 3D high Reynolds number turbulent boundary layer with proper resolution of the micro holes is beyond the current and perhaps future computational capability. An alternate method that has the potential for such a study is based on large-eddy simulations (LES). In LES, all scales larger than the grid are resolved in a space and time accurate manner and only the scales smaller than the grid are modeled using a subgrid model. We have developed an advanced localized dynamic model based on the subgrid kinetic energy (Menon et al. [9–12]) that has shown to be very accurate even when relatively coarse grid is employed. This ability has some significant implications when high Reynolds number flows have to be simulated, as required under this project.

Although LES looks promising, it has a serious problem in near-wall flows. To properly resolve the small-scale dynamics in the log layer, the wall normal resolution has to be close to the DNS requirement. This implies that the computational cost will be unacceptable. Clearly, an alternate method is required.

In another recent study (Menon [13–15]; Menon and Wang [16]), a simulation methodology based on the Lattice Boltzmann Equation (LBE) was developed and demonstrated for the study of synthetic MEMS jets (e.g., Smith and Glezer [17]) embedded inside typical fuel jets. Both the synthetic jet cavity and the fuel jet are modeled using the same solver and thus, no specific imposition of boundary conditions at the synthetic jet exit (as done in the past) is required. The unique feature of the LBE approach is that it solves the Boltzmann equation (which, in the continuum limit recovers the Navier-Stokes equation). Since the Boltzmann equation is a single scalar equation, it is computationally very efficient (in fact, orders of magnitude faster than conventional FV algorithm). Thus, very high resolution (in fact, DNS-like resolution) can be used in the LBE model without paying a price in terms of computational cost.

In the present study, the LBE model is being developed for use primarily to resolve the flow field inside the air injectors while the conventional FV-LES model is being used to simulate the boundary layer flow. This approach takes the best of both worlds and couples them together within a single formulation. The LBE solver is fully coupled to the LES solver and interacts across block structured grid domains. Thus, in the injection/suction port regions and in the near wall region (e.g., below  $y^+ < 200$ ), a high (DNS-like) resolution will be used and the flow field simulated (without requiring any modeling, and this is important!!) using the LBE model, while in regions away from the wall, a conventional FV LES code will be employed.

This report summarizes the work accomplished over the period of January 2002 to September 2002 under this project. Significant accomplishments have been achieved over the last 8 months.

## 2. Technical Objectives

This project has the following overall technical objectives for the **3-year** project:

1. Demonstrate the LES-LBE model for simulation of the turbulent boundary layer and the micro-scale blowing system in a seamless coupled manner.

This is the primary objective of the present year's effort. The focus so far has been on developing a baseline LBE model for a single injection system and then to scale it to simulate multiple injection ports. Effort has also focused on setting up a FV LES solver to simulate the subsonic boundary layer currently being investigated experimentally at NASA GRC

2. Apply the LES-LBE solver to flows identified by NASA GRC in order to validate the methodology and to understand the physics of the interaction process.

The exact configuration and test conditions to be used for validation has been chosen in collaboration with researchers at NASA GRC. Initially, we are studying micro-blowing in a Mach 0.4 subsonic turbulent boundary layers. Subsequently, micro-blowing in supersonic flow will be considered in the second and third years.

3. Employ the LES-LBE model to study new strategies and to provide researchers at NASA with more detailed information on the dynamical processes that are occurring during micro-blowing and/or suction.

Once the baseline code has been validated, we plan to simulate additional scenarios that may or may not have been experimentally evaluated. The choice of conditions (e.g., steady or unsteady) and geometry to be simulated will be determined in close collaboration with NASA GRC research team. The primary objectives here are to determine if the simulation tool can be used to fine-tune and optimize existing setups that have already been experimentally evaluated at NASA GRC, and then to use the tool to investigate new conceptual designs. Once a representative new configuration is determined, experimental evaluation of the design will be addressed. We expect this effort to be on-going during this research program.

4. Further demonstrate the ability of the LES-LBE solver to study more complex micro-blowing/suction strategies for drag control.

Although the experiments at NASA GRC have primarily evaluated micro-blowing techniques, combined blowing and suction could also be a method for drag control. Simulation of combined blowing and suction using the LES-LBE technique will be considered in the latter half of the second year. This may lead to a new capability to study drag control (i.e., increase or decrease drag on-demand).

5. Carry out a focused set of experimental studies (in Georgia Tech's Mach 2.5, 8 cm x 10 cm test section boundary layer facility) of micro-scale blowing/suction in a supersonic boundary layer to obtain data LES validation.

We have a supersonic test facility at Georgia Tech (Fernando and Menon [18]) that will be used in the second year to obtain some baseline data for LES validation in the supersonic regime. Detailed measurements using LDV, pressure pitot probes and PLIF are planned. All capabilities are currently operational in our lab.

### 3. Summary of Accomplishments To-Date

This project actually started in late January 2002 at Georgia Tech and the highlights noted below are for the **first 8 months of this research**.

#### ***[1] 3D LBE-LES solver for simulating injection developed and validated.***

This is a key objective since in the present study, the injection port all the way to the upstream controller will have to be simulated because the flow in the vicinity of the port hole cannot be prescribed a priori due to complex interactions. Furthermore, the flow field in this vicinity has to be relatively well resolved. Therefore, a new 3D LBE-LES approach has been developed to simulate the flow inside the injection port. In order to ensure its accuracy, simulations were carried out for a single port injection into a cross-stream. Results have been compared to experimental data and very good agreement has been obtained (in fact, superior to RANS two-equation and Reynolds-Stress closure models). These results have established the accuracy of the 3D LBE model as implemented in the LES mode.

#### ***[2] LES of Incompressible and Compressible Channel Flows***

This is another critical objective since we need to demonstrate the accuracy of the LES solver to capture the baseline boundary layer in the experimental studies at NASA GRC. Since the flow is at a Mach number of 0.4, fully compressible LES solver has been developed for this purpose. Again, to this validation phase, we are simulating two test cases: (a) LES of an incompressible channel flow for which detailed DNS data is available (Moser et al. [19]), and (b) LES of a compressible channel flow with parameters that match the experimental set up of NASA GRC. The former test case will address the resolution and accuracy of the code against a well-documented database. However, this DNS database is at a relatively low Re ( $Re = 590$  based on wall units) and therefore, the second task is focusing on the actual experimental condition, which is at a very high Re. Since there are only limited measurements, we are using the DNS data to validate the base code. The comparisons obtained so far show that our LES code is quite accurate and sufficient to ensure accuracy of the flow physics of interest. This task and the task of LES of the experimental flow case are both underway and final results are expected in the near future. It is, however, anticipated the validation of the LES solver for flows of current interest will be accomplished within the next 2 to 3 months.

#### ***[3] New Near-Wall and Injection Port Subgrid Modeling***

In parallel to above studies, a new effort is being initiated that leverages on the recent development of a new near-wall model for LES (funded by Office of Naval Research). In this approach, the region near the wall and the small-scale turbulence field are simulated in another embedded locally 1D grid that retains DNS-level accuracy but is computationally much cheaper. This approach therefore, employs a grid-within-grid approach whereby the large-scales are simulated using conventional LES while the small-scales are simulated using local 1D grids. Preliminary results for channel flow have been obtained with very

good accuracy. The idea here is to implement this local 1D model in the injection port all the way to the upstream controller. This approach differs from the LBE approach (see [1] above) in that, the LBE approach is fully 3D but in phase space whereas this subgrid 1D approach is implemented completely in physical space and is coupled directly to the LES solver.

It is worth noting that this approach is very new and still needs some major development (some of which is currently being carried out in a parallel ONR project) but has the potential to capture the physics all within a single LES formulation.

#### ***[4] Methodology to simulate a large-number of injection ports simultaneously***

Finally, since the goal is to simulate 100 to 10000 holes simultaneously without specifying boundary condition at the injection port, some new issues need to be explored. We have begun this effort and have developed the basic framework for simulating many ports simultaneously. Both locally 1D (using the approach noted in [3]) and fully 3D (using LBE) are being setup. We expect to get some preliminary results within the next 2 months using both these methods after which one of them will be chosen for more careful simulations.

## **4. Numerical Tools**

For completeness we are summarizing the key codes being used in the present effort.

### **4.1 Finite-Volume LES Solver**

A fully compressible, unsteady, finite-volume LES solver that is second-order accurate in time and fourth-order accurate in space is employed for all the simulations of the boundary layer flow. This code has been extensively employed to study turbulent flows, fuel-air mixing, premixed, non-premixed and spray combustion in complex domains as in full-scale gas turbine and internal engine combustors. The code has been highly optimized for parallel processing. To simulate flows with shock waves, a second order flux vector splitting scheme is also implemented in the code. A localized dynamic subgrid model based on the transport model for the subgrid kinetic energy is used to close the LES subgrid terms. Details are given in cited references [10, 12, 20]. The key advantage of this closure model is that since the subgrid velocity scale is explicitly computed (the length scale is still approximated based on the grid scale), the assumption of local equilibrium between subgrid kinetic energy production and dissipation (that is inherent in algebraic subgrid eddy viscosity models) does not have to be imposed. As a direct result, this subgrid model allows simulation high-Re flows using relatively coarse grids without compromising the accuracy of the prediction of the large-scale processes since the non-equilibrium effects in the small-scales are incorporated within the subgrid model. Finally, the dynamic evaluation used in this model employs a scale-similarity approach, which avoids the limitations of the Germano's dynamic closure and thus, is more robust and applicable in complex flows without requiring ad hoc averaging or smoothing.

## 4.2 LES-LBE Solver

Since the LES-LBE model is a relatively new development it is described in some detail below. LBE method originates from a Boolean fluid model known as the lattice gas automata (LGA) which simulates the viscous fluid flow by tracing the fluid motion through advection of fluid particles and particle collision on a regular lattice. LBE is an improvement over LGA in which the Boolean fluid model is replaced by a single continuous particle distribution, which is analogous to the particle distribution function in kinetic theory. This replacement eliminates the intrinsic noise inherent in LGA schemes and overcomes the shortcomings of a limited transport coefficient. The introduction of the BGK single relaxation time model for the collisional operator further simplifies the algorithm and eliminates the lack of Galilean invariance and the dependence of pressure on velocity [21, 22]. This model assumes that the particle distribution function relaxes to its equilibrium state at a constant rate, and the collision operator is similar to the classical BGK Boltzmann operator (Bhatnager et al. [23]).

Whereas conventional Navier-Stokes schemes solve the macroscopic properties of the fluid explicitly, LBE method solves the Boltzmann equation by tracking the evolution of the microscopic particle distribution of the fluid. The conserved variables of the fluid (density and momentum) are obtained indirectly by local integration of the particle distribution. The incompressible Navier-Stokes is recovered in the nearly incompressible limit of LBE using the Chapman-Enskog expansion. Solving the lattice Boltzmann equation instead of the Navier-Stokes equation provides three distinct advantages. First, due to the kinetic nature of the LBE method, the convection operator is linear. Simple convection in conjunction with a collision process allows the recovery of the nonlinear macroscopic advection through multi-scale expansions. Second, since the macroscopic properties of the flow field are not solved directly, LBE method avoids solving the Poisson equation, which proves to be numerically difficult in most finite difference methods. Third, the macroscopic properties are obtained from the microscopic particle distributions through simple arithmetic integration. More details are given in a recent review (Chen and Doolen [24]).

### 4.2.1 The Lattice Boltzmann Equation Model

LBE method consists of two primary steps. The particles first stream to its next nearest neighbor in the direction of its prescribed velocity. Subsequently, particles of different velocity arriving at the same node interacts with each other by relaxing to its local equilibrium values which are formulated specifically to recover the low Mach number limit of the Navier-Stokes equation. The evolution of the distribution function  $f_\alpha$  is thus govern by:

$$f_\alpha(x + e_\alpha \delta, t + \delta) - f_\alpha(x, t) = \frac{1}{\tau} [f_\alpha^{eq}(x, t) - f_\alpha(x, t)], \alpha = 0, 1, \dots, 18 \quad (1)$$

where  $\tau$  is the relaxation time,  $f_\alpha^{eq}$  is the equilibrium distribution function and  $e_\alpha$  is the particle speed in  $\alpha$  direction. The characteristic speed is thus  $c = e_\alpha \delta / \delta = |e_\alpha|$ . Rest particles of type 0 with  $e_0 = 0$  are also allowed. Note that the time step and the lattice spacing each have equal spacing of unity. Thus,  $\delta = 1$  in the above formulation.

In principle, there are an infinite number of possible velocity directions in the 3D velocity space. Discretizing these infinite number of velocity directions into a fixed set of velocity directions inevitably introduces discretization errors to the solution. As a general rule, the accuracy of the model to simulate Navier-Stokes flow comes at the expense of increasing computational cost resulting from the number of discrete velocities used in the model. Frisch et al. (1986) have shown that the Navier-Stokes equation cannot be recovered unless sufficient discrete velocities are used to ensure lattice symmetry.

There are various 3D cubic lattice models developed, most notably the 15-bit (D315), 19-bit (D3Q19), and 27-bit (D3Q27) model [26]. Here, using common notations in scientific literatures, D is the number of dimensions and Q is the number of discrete velocities. In previous numerical simulations of a square duct, a lid-driven cavity and a circular pipe [27] no significant improvement in accuracy is observed when the D3Q27 model was used over the D3Q19 model and thus, the latter model is assumed to be sufficient for the current purpose.

The 19-bit velocity field is given as:

$$e_\alpha = \begin{cases} (0,0,0) & \alpha = 0, \text{ rest particle} \\ ((\pm 1,0,0), (0,\pm 1,0), (0,0,\pm 1))c & \alpha = 1, 2, \dots, 6, \text{ class I links} \\ (((\pm 1,\pm 1,0), (0,\pm 1,\pm 1), (\pm 1,0,\pm 1))\sqrt{2}c & \alpha = 7, 8, \dots, 18, \text{ class II links} \end{cases} \quad (2)$$

Here,  $f_\alpha^{eq}$  is given by the following form:

$$f_\alpha^{eq} = w_\alpha \rho \left[ 1 + \frac{3(e_\alpha \cdot u)}{c^2} + \frac{9(e_\alpha \cdot u)^2}{2c^4} - \frac{3u^2}{2c^2} \right], \quad (3)$$

where

$$w_\alpha = \begin{cases} \frac{1}{3} & \alpha = 0 \\ \frac{1}{18} & \alpha = 1, 2, \dots, 6 \\ \frac{1}{36} & \alpha = 7, 8, \dots, 18 \end{cases}$$

The macroscopic properties of the flow field can be obtained by integrating the distribution functions over the velocity space:

$$\rho = \sum_{\alpha} f_{\alpha} \quad (4)$$

$$\rho u = \sum_{\alpha} e_{\alpha} f_{\alpha} \quad \alpha = 0, 1, \dots, 18 \quad (5)$$

Here,  $\rho$  is the density and  $u$  is the velocity.

The Navier-Stokes mass and momentum equations obtained using the BGK single relaxation time model by employing Chapman-Enskog on Eq.(1) are:

$$\frac{\partial \rho}{\partial t} + \frac{\partial \rho u_{\alpha}}{\partial x_{\alpha}} = 0 \quad (6)$$

$$\frac{\partial(\rho u_{\alpha})}{\partial t} + \frac{\partial(\rho u_{\alpha} u_{\beta})}{\partial x_{\beta}} = \frac{\partial(c_s^2 \rho)}{\partial x_{\alpha}} + \frac{\partial(2\nu\rho S_{\alpha\beta})}{\partial x_{\beta}} \quad (7)$$

Here, repeated indices indicate summation and  $S_{\alpha\beta} = \frac{1}{2}(\partial_{\alpha}u_{\beta} + \partial_{\beta}u_{\alpha})$  is the strain-rate tensor. The pressure is given by the constant temperature ideal gas equation of state  $p = c_s^2 \rho$  where  $c_s$  is the speed of sound with ( $c_s = c/\sqrt{3}$ ), and  $\nu = [(2\tau - 1)/6]$  is the kinematics viscosity.

#### 4.2.2 Subgrid Scale Modeling in LBE Formulation

Since our eventual interest is in the application of the LBE model within the LES approach, the above formulation needs to be extended to LES. Spatial filtering reduces the high wave number Fourier components of the particle distribution and separates the resolved scale parts from the unresolved scales. For high Reynolds flow, LES-LBE formulation results in the "filtered" form of the LBE equation (LES-LBE):

$$\overline{f_{\alpha}}(x + e_{\alpha}\delta, t + \delta) - \overline{f_{\alpha}}(x, t) = \frac{1}{\tau_{sgs}} \left[ \overline{f_{\alpha}^{eq}}(x, t) - \overline{f_{\alpha}}(x, t) \right], \alpha = 0, 1, \dots, 18 \quad (8)$$

Here, the distribution function  $\overline{f_{\alpha}}$  represents only those of the resolved scales. The effect of the unresolved scale motion is modeled through an effective collision term:

$$\nu + \nu_{\tau} = \frac{2\tau_{sgs} - 1}{6} \quad (9)$$

The eddy viscosity  $\nu_\tau$  represents the effect of dissipation by the unresolved scales and must be modeled. In the present effort, we have investigated the application of a simple algebraic model based on the classical Smagorinsky's model:

$$\nu_\tau = C_\nu \Delta^2 S \quad (10)$$

where  $C_\nu$  is the Smagorinsky constant,  $\Delta = (\Delta_x \Delta_y \Delta_z)^{\frac{1}{3}}$  is the associated length scale derived from the local volume of the lattice and  $S = (2\overline{S_{ij}S_{ij}})^{1/2}$  is the characteristic filtered rate of strain.

The constant in Eq. 10 is unknown and cannot be prescribed a priori. Therefore, a localized dynamic method (LDM) [10, 12] is used to compute this ‘‘constant’’ locally as a function of space and time. The LDM is formulated based on the assumption of scale similarity in the inertial subrange and provided that enough of the inertial subrange is resolved, stresses at the cutoff (i.e., the grid size) can be related to stresses at say, twice the cutoff (i.e., the test filter width). This then defines a scale level where explicit filtering is required. The test-scale field is constructed from the grid-scale field by applying a test filter, which is characterized by  $\hat{\Delta}$  (typically,  $\hat{\Delta} = 2\bar{\Delta}$  and  $\bar{\Delta}$  is the characteristic grid size). Thus, the application of the test filter on a variable  $\phi$  is denoted by  $\hat{\phi}$  and the test-scale Favre-filtered variable is denoted by  $\langle \phi \rangle = \bar{\rho} \hat{\phi} / \hat{\rho}$  and  $C_\nu$  is obtained using the relation (see Kim and Menon [10] for more details)

$$C_\nu = \frac{L'_{ij} M_{ij}}{2M_{ij} M_{ij}} \quad (11)$$

Equation (11) is an overdetermined system and is solved using a least-square method. In the above equation,  $L'_{ij} = L_{ij} - \frac{2}{3} \hat{\rho} k^{test} \delta_{ij}$ ,  $M_{ij} = -\hat{\rho} \sqrt{k^{test}} \hat{\Delta} \left( \langle \tilde{S}_{ij} \rangle - \frac{1}{3} \langle \tilde{S}_{kk} \rangle \delta_{ij} \right)$ , and  $L_{ij} = \hat{\rho} \left( \langle \tilde{u}_i \tilde{u}_j \rangle - \langle \tilde{u}_i \rangle \langle \tilde{u}_j \rangle \right)$  is the Leonard stress tensor. Also,  $k^{test} = \frac{1}{2} \left( \langle \tilde{u}_i \tilde{u}_j \rangle - \langle \tilde{u}_i \rangle \langle \tilde{u}_j \rangle \right) = \frac{1}{2} \frac{L_{kk}}{\hat{\rho}}$  is the resolved kinetic energy at the test-filter level and  $\tilde{S}_{ij} = \frac{1}{2} \left( \frac{\partial \tilde{u}_i}{\partial x_j} + \frac{\partial \tilde{u}_j}{\partial x_i} \right)$  is the resolved-scale rate-of-strain tensor.

### 4.2.3 Boundary Conditions

The most commonly used method to apply a no-slip boundary condition is the particle bounce-back scheme: the particles arriving at the stationary wall are reflected back in the direction it came from. Although easy to implement, the exact location of the no-slip wall is in question. The bounce-back scheme exhibited second order accuracy when the no-slip wall is placed at exactly halfway between the boundary node and the

first fluid node in numerical simulations of Poiseuille flow using the D2Q9 and D3Q15 models (Zou and Hem[28]). Thus, the 3D adaptation of this bounce-back boundary condition from the D2Q6 model [29] to the present D3Q19 model [30] used for this study is assumed to be adequately accurate. It has been noted that certain wall geometries (e.g. convex edge and convex corner) cannot satisfy the no-slip condition under this scheme because there are insufficient unknown populations to define such a condition, resulting in curved instead of sharp-edged boundary.

For orifice boundaries, a new treatment is proposed whereby, the no-slip wall is embedded within the grid and the unknown population of the inward pointing link with vector  $e_{\bar{\alpha}}$  is computed prior to streaming by:

$$f_{\bar{\alpha}}(x_b, t) = (1 - \chi)f_{\alpha}(x_f, t) + \chi f_{\alpha}^*(x_b, t) + 2w_{\alpha}\rho \frac{3}{c^2} e_{\bar{\alpha}} \cdot u_w \quad (12)$$

Here, subscripts  $b$ ,  $f$  and  $w$  denote the boundary node, fluid node and the embedded wall, respectively, and  $\alpha$  denotes the opposite outward pointing link (i.e.  $e_{\alpha} = -e_{\bar{\alpha}}$ ). Here,  $f_{\alpha}^*$  is an extrapolated population defined by:

$$f_{\alpha}^* = \omega_{\alpha}\rho(x_f, t) \left[ 1 + \frac{3}{c^2} e_{\alpha} \cdot u_{bf} + \frac{9}{2c^4} (e_{\alpha} \cdot u_f)^2 - \frac{3}{2c^2} u_f \cdot u_f \right] \quad (13)$$

where,

$$u_{bf} = \left[ 1 - \frac{3}{2\Delta} \right] u_f + \frac{3}{2\Delta} u_w \quad \text{and} \quad \chi = \frac{2\Delta - 1}{\tau + 1/2} \quad \text{for } \Delta \geq 1/2 \quad (14)$$

$$u_{bf} = u_{ff} = u_f(x_f + e_{\bar{\alpha}}\delta, t) \quad \text{and} \quad \chi = \frac{2\Delta - 1}{\tau - 2} \quad \text{for } \Delta < 1/2 \quad (15)$$

Here,  $\Delta$  is the fraction of an intersected link in the fluid region. More details are given elsewhere.

## 5. Progress to Date

In this section, we present our recent results and progress in this project. The progress in each of the topics highlighted in Section 3 is discussed in separate sections. As noted earlier, these results have been obtained over the first 8 months of the first year.

### 5.1 LES-LBE Studies of Jet in Cross-flow

In order to validate the sub-grid model a square jet in cross-flow has been simulated. The experiment of Ajresch et al. [31]

is chosen as the benchmark case for validation studies and the dimensions of the computational domain is shown in Fig. 1. The simulation is carried out at Reynolds number of 4700 based on the jet velocity and the nozzle width  $D$  and at jet-cross-flow velocity ratio of 0.5. The crossflow velocity profile is initialized with a boundary layer thickness of  $2D$ . The computational domain is resolved using  $200 \times 50 \times 100$  for the cross-flow domain and  $50 \times 50 \times 100$  for jet section. The simulation required approximately 1.84GB of memory and 1500 single processor hours on SGI O2000. Note that to do this simulation using conventional FV scheme the computational cost will easily exceed this number by more than an order of magnitude. Periodic boundaries are used in the cross-stream boundaries of the cross-flow domain to simulate a single square jet out of a row of six used in the experiment. On the top surface free slip and for exit surface, outflow conditions have been implemented.

The incoming pipe velocity profile with constant value is prescribed in the pipe at a distance of  $10D$  below the flat plate allowing the flow to develop naturally as the jet merges into the cross-flow. This is a key requirement for the present project. The mean velocity profile comparisons are presented at various streamwise stations  $x/D$  along the jet center plane  $y/D = 0$  and along the edge of the jet  $y/D = -0.5$  in Figs. 2 and 3. Results obtained earlier using the standard  $k - \epsilon$  model (Lam and Bremhorst [32]), and more complex Reynolds-stress closure [33, 34] are also included for comparison. It can be clearly seen that the present LBE results are considerably superior to these earlier attempts for this flow.

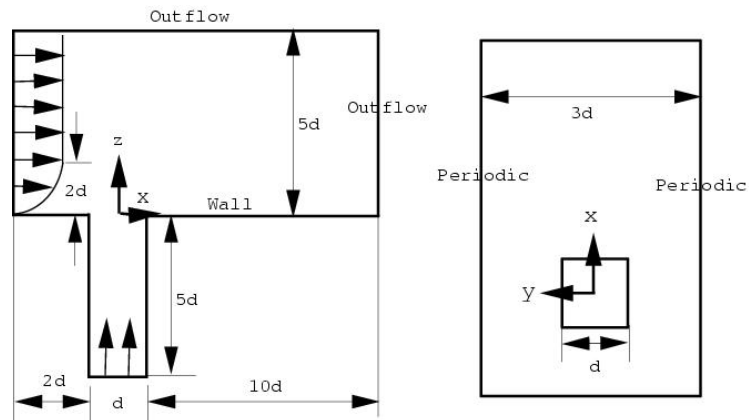


Figure 1. Geometry and computational domain employed in this study

Figure 4a shows the iso-surface of vorticity structures in vertical, spanwise and streamwise direction. The green isosurface marks regions in the flow where  $|\omega_x| = 0.003$ , the blue surface marks the same magnitude for  $|\omega_y|$  and the red surface marks the same magnitude for  $|\omega_z|$ . These structures have been called hanging vortices ( $\omega_x$ ), spanwise rollers ( $\omega_y$ ) and vertical streaks ( $\omega_z$ ) [35] due to their distinctive characteristics. The hanging vortices are tube-like structures that begin directly above the exit on the lateral edges of the jet and then extend around the jet body and then up along the backside of the jet roughly matching the jet trajectory. Thus, these tubes mark the location where the jet shear layer rolls up into a vortex tubes and eventually contribute to the circulation of the counter-rotating vortex pair (CVP). Directly above the jet exit in Fig. 4 two vertical structures are clearly evident. One begins directly at the exit on the lateral edge of the jet and extends up and around the jet body while the second is located downstream above the first and extends horizontally along the lateral edge of the jet. Hanging vortices provides a path downstream for the jet fluid.

Figure 4b shows two sets of instantaneous streamlines. One set originates within the jet, and the second set originates from the crossflow boundary layer upstream of the jet exit. These lines also collect in the hanging vortex. The vorticity carried by the hanging vortex provides the circulation necessary to create CVP. The CVP changes position and strength with time and streamwise location.

Vertical streak forms when the irregularities in the rollers are stretched vertically by the local strain field. The majority of the production of vertical streaks occurs in the upstream rollers. The vorticity magnitude and streamlines are shown in Figs. 6a and 6b. It can be seen that the complex vortex pattern form downstream of the jet as it turns towards the direction of the flow.

The present simulation of jet in crossflow has shown good agreement with experiments. Furthermore, the ability of the LES-LBE approach is observed to be superior to the previous RANS studies. In addition, the LES-LBE simulation also provides a means to study the unsteady dynamics of the mixing process. A movie is attached to this report that shows this complex unsteady dynamics.

The baseline study has established the ability and accuracy of the LES-LBE approach. Therefore, we are now ready to implement this model within conventional LES to simulate the multiple injection port. Note that for this coupled effort we are interested in only simulating the injection region with LBE. Also, the resolution requirement within the injection port does not have to be as high as in the present study since the scale of the injection hole is much smaller than the square port simulated here. Also, we have extended this LBE model to simulate circular and elliptical shaped holes as well. Therefore, all elements are ready for coupling to the LES code and will be the focus of the last quarter of this year's effort.

However, before attempting the fully coupled simulation, it is also necessary to demonstrate the accuracy of the LES solver for this type of flow. To do this we have carried out controlled LES of turbulent channel flows, both for a case for which DNS detailed data is available and another case which corresponds identically to the test case being measured at NASA GRC. These studies are discussed in the next section.

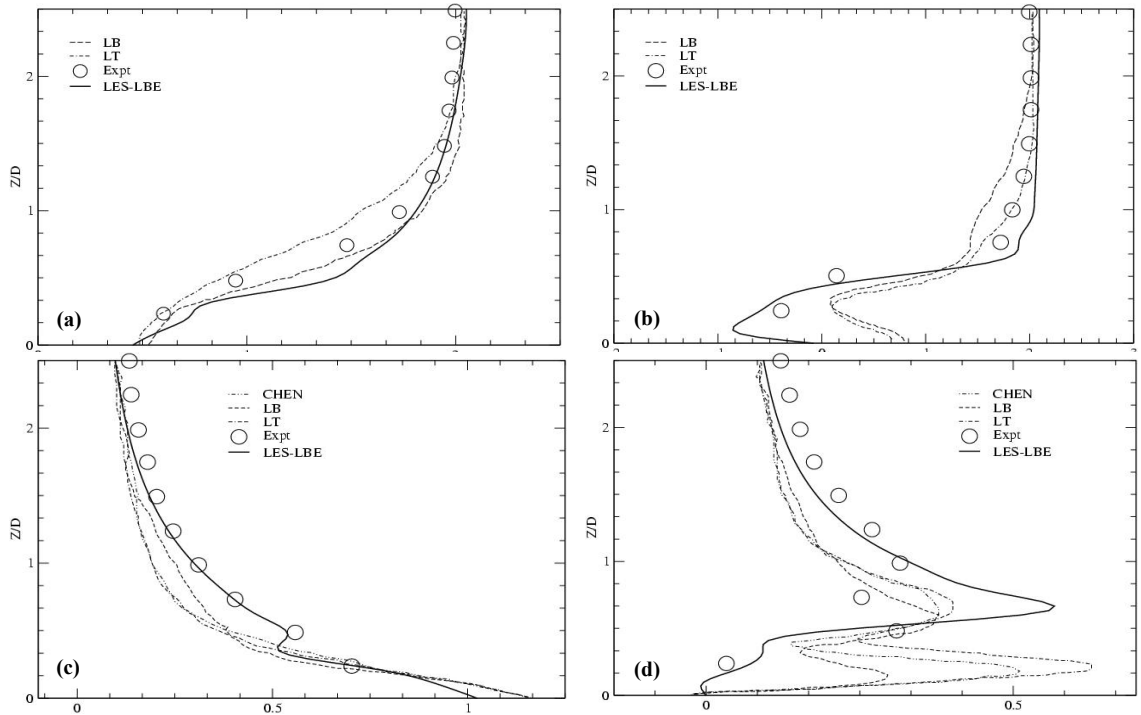


Figure 2. Comparison of LES-LBE predictions of velocity profiles with past RANS results and experimental data at jet centerline. Figures (a) and (b):  $U/W_{ref}$  at  $x/D=0$  and 1, (c) and (d):  $W/W_{ref}$  at  $x/D=0$  and 1.

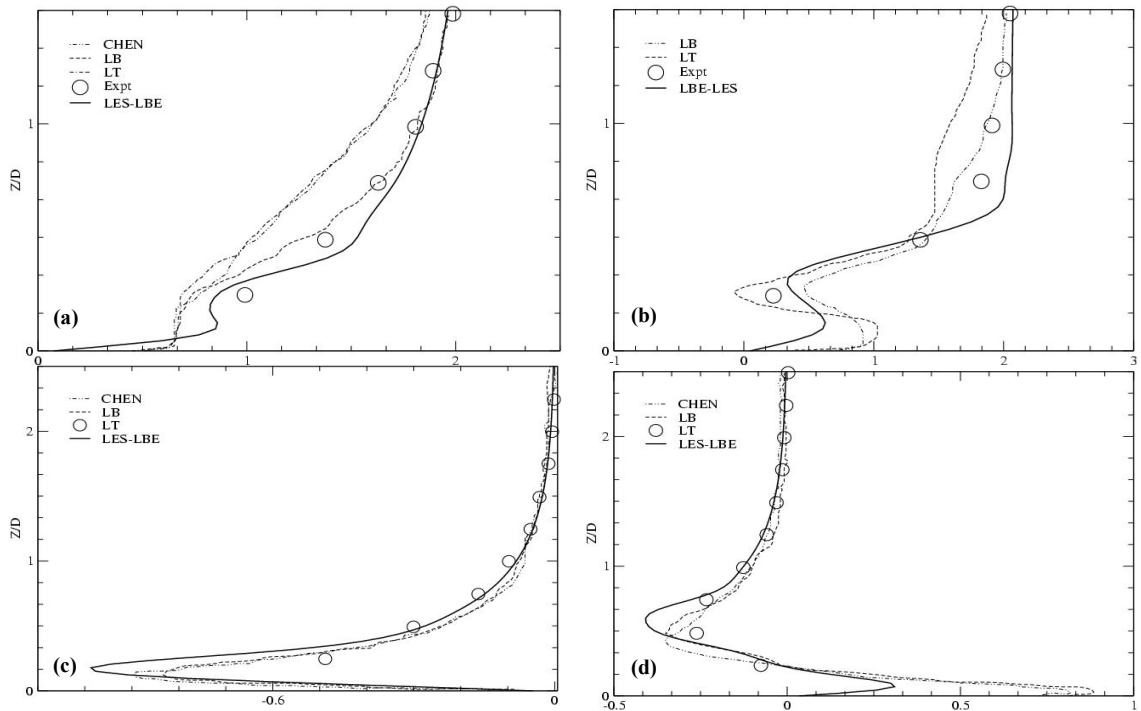


Figure 3. Comparison of LES-LBE predictions of velocity profiles with past RANS results and experimental data at jet edge. Figures (a) and (b):  $U/W_{ref}$  at  $x/D=0$  and 1, (c) and (d):  $W/W_{ref}$  at  $x/D=0$  and 1.

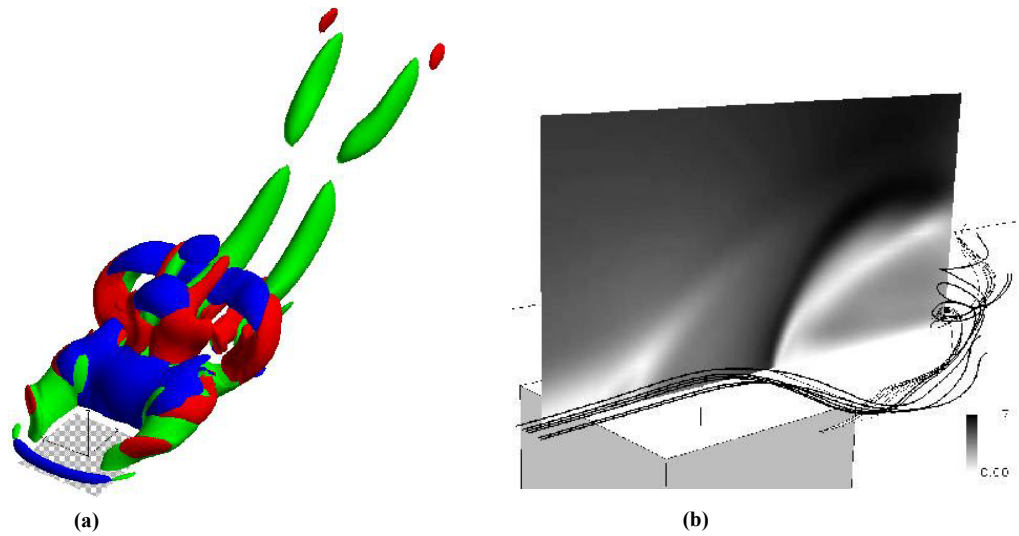


Figure 4. Characteristics flow pattern in jet in cross-flow. (a) Vorticity contours showing the various components, (b) Streamline pattern from the free stream and the injected jet.

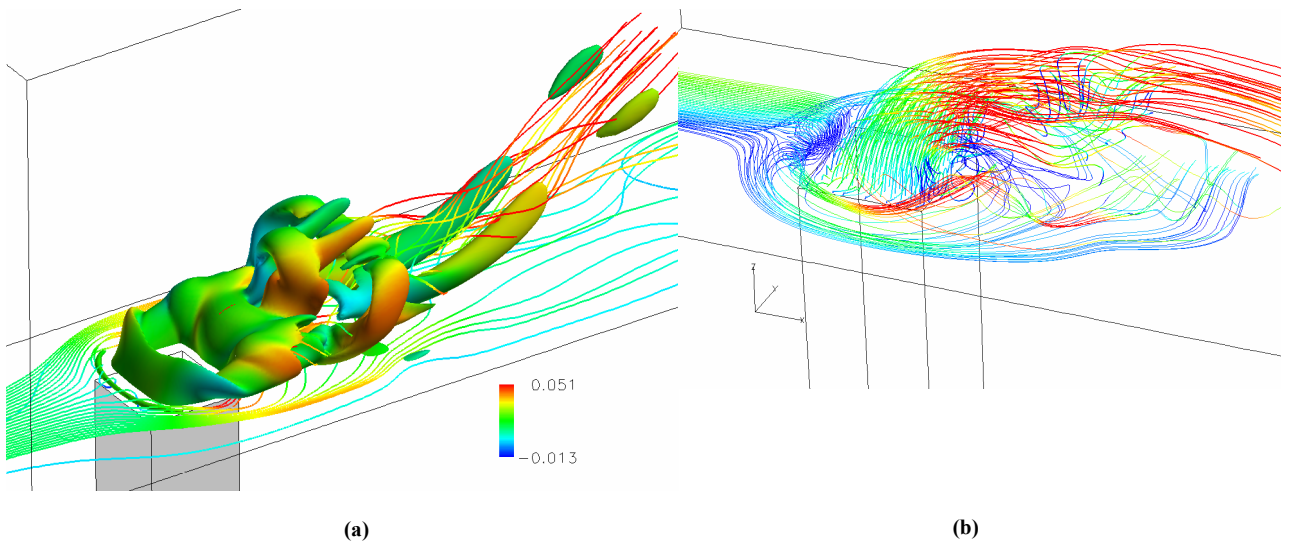


Figure 5. Instantaneous vorticity and streakline patterns in the jet in cross-flow. Vortex rollup and breakdown, followed by the formation of the kidney-shaped structure in the downstream side is clearly seen. Recirculating flow in the wake of the jet is also clearly seen. All observations are in good agreement with experimental observation.

## 5.2 3D Channel Flow for LES Validation

In order to validate the LES code, numerical simulations of channel flow for  $Re_\tau = 590$  were performed. This test case was chosen since a detailed DNS analysis has been carried out in the past [19] and therefore, detailed database is available for validation. This test case is for low-speed incompressible flow but our compressible code can handle this limit and therefore, this test case was chosen for code validation. Figure 6 shows the configuration and dimensions that have been used for this simulation. Periodic boundary conditions are applied in the stream-wise (x) and span-wise directions. The inflow velocity of 19.68 with  $\delta = 0.01$  was considered for this case. The computational domain is resolved using  $64 \times 128 \times 64$  point in x, y and z directions for the current dynamic LES studies. In contrast, the DNS studies of Moser et al. [19] employed a resolution of  $387 \times 256 \times 256$ .

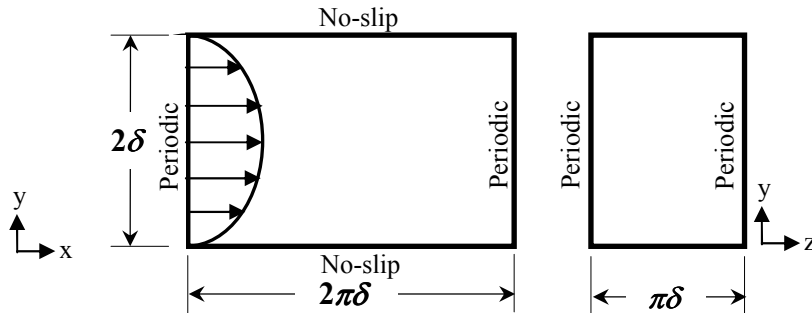


Figure 6. Dimensions and boundary conditions used for channel flow

The profile of the mean velocity normalized by the wall-shear velocity is shown in Fig. 7. Within the sub-layer ( $y^+ < 5$ ) the computational results follow the linear law ( $U^+ = y^+$ ) of the wall and in the logarithmic region, the log law holds. Turbulence intensities normalized by the wall-shear velocity are shown in Fig. 8. This simulation is still underway but preliminary comparison looks very good. More detailed comparison will be carried in the near future but results show far show that the current LES model is accurate enough to be applied to the micro-blowing study.

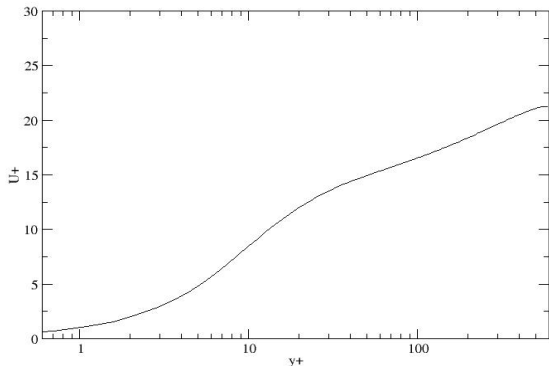


Figure 7. Mean velocity profile in wall unit

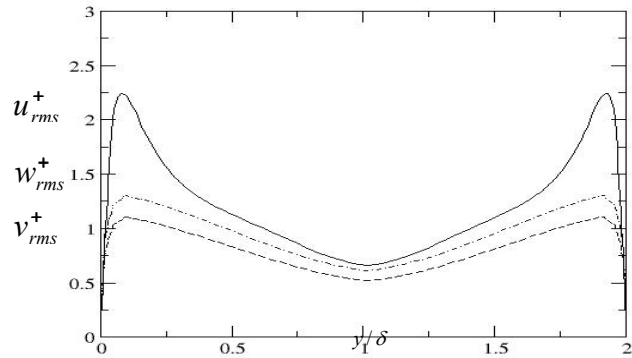


Figure 8. Root-mean square velocity fluctuations normalized by the wall shear velocity

### 5.3 LES of subsonic boundary layer on a flat plate (NASA GRC experiment)

The study in Section 5.2 has established the baseline code but it was for a low speed (incompressible) flow condition. We have also set up the NASA GRC test case for validation as well. However, since very limited data is available only integrated parameters will be compared. Although it is believed that the present code is accurate enough to capture the dynamics of the high Re flat plate boundary layer simulated in the experimental study we still need to establish this prior to the micro-blowing simulations. Air flow past the flat plate with temperature of 284 K, pressure of 27068 Pa and an inflow velocity is 145.3 m/s ( $M=0.3$ ). Figure 9 shows the geometry of this simulation. The boundary layer thickness is 3.5 cm and a  $128 \times 256 \times 128$  grid has been used for the present study. The grid is highly stretched near the wall to resolve the near wall region.

This simulation is still underway but the results are expected within the next month. Note that our code is highly optimized for parallel simulation. However, we do not have access to NASA parallel machines for these studies. We are currently using a 32-processor cluster in our lab for this simulation. We are also testing a new 64-processor PC (Intel Pentium IV Xeon) cluster in our lab. This cluster has been built with this project in mind. Once this machine is on-line we hope to speed up the calculations.

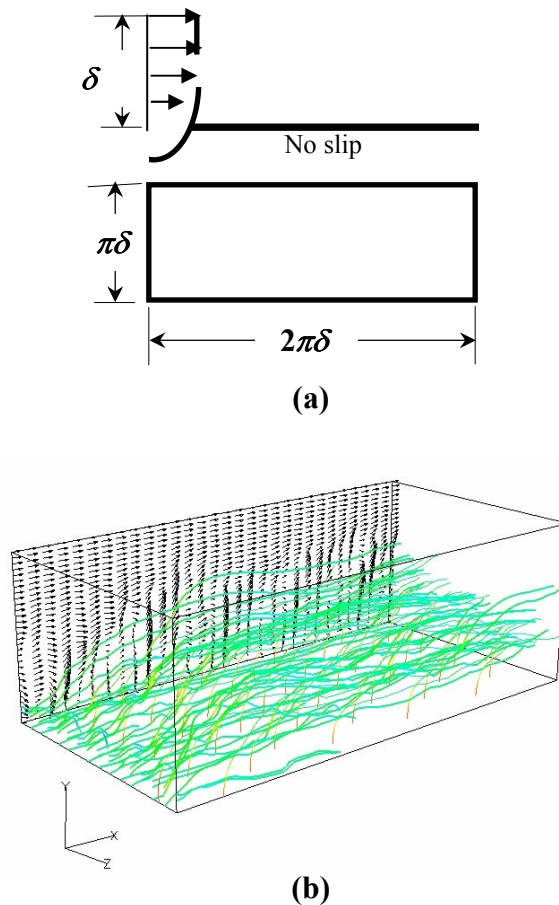
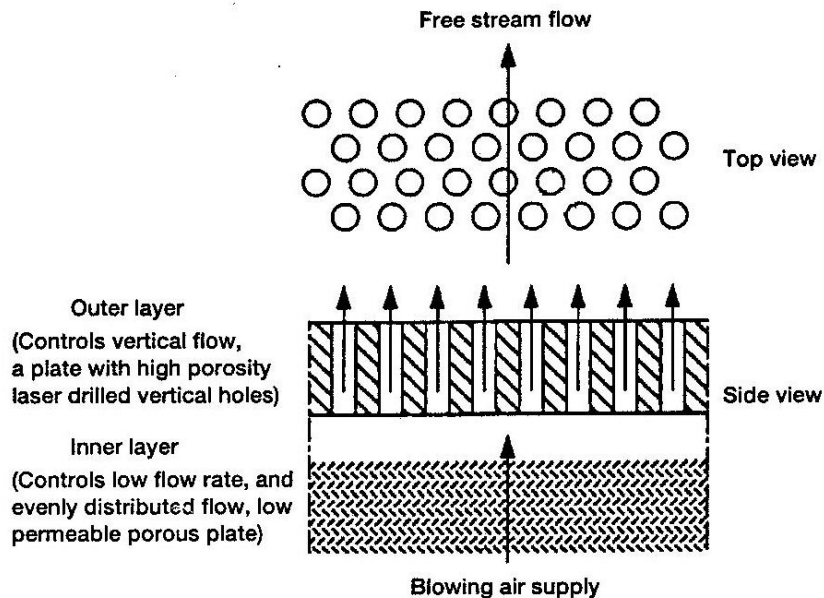


Figure 9. Schematic of the computational domain used to model the experimental setup at NASA GRC. Figure below show a preliminary flow pattern in the channel.

## 5.4 Simulation Methodology to Simulate Micro blowing

Given that the LBE approach and the LES solver are operational, the next step is to determine how to simulate 100 to 1000 of injection micro-holes within a single simulation. Such a study has never been attempted in the past and it offers some interesting challenges. Some important conditions have to be maintained and these are discussed (along with method of study) in the following.

All the injection holes have to be simulated simultaneously, as in the real experiment. This is schematically shown in Figure 10. In the experiments, an extremely small amount of air is blown vertically through these very small holes. However, the flow condition is determined by the upstream stagnation or control condition. In order to capture the proper dynamics in the boundary layer region, it is necessary to simulate from the upstream condition and also through the injection tubes. We plan to investigate two approaches that do NOT compromise or drastically increase the computational cost. The first approach is the method based on the LBE model discussed above. The second approach is more innovative but is also a new approach that was recently developed under a ONR project for high Re boundary layer flows but still needs to be evaluated for the present application in highly compressible flow. The second approach is discussed briefly in the next section.



**Figure 10. Micro-Blowing configuration in the experiment**

To simulate the multi-port blowing section two methods are being investigated. A schematic diagram of micro-blowing simulation is shown in Fig. 11. The issue here is to ensure that all the ports are resolved reasonably well and also that upstream conditions

can be prescribed on all ports as done in the experiment. The two approaches being implemented are (a) the LBE approach discussed in section 5.1 and the new locally 1D approach (discussed below in the next section). The LBE approach is mature and therefore, can be considered for implementation at this stage. However, the subgrid 1D approach will require more development (some of which is still underway in the ONR project), especially for highly compressible flow. However, we will look at both approaches in some detail.

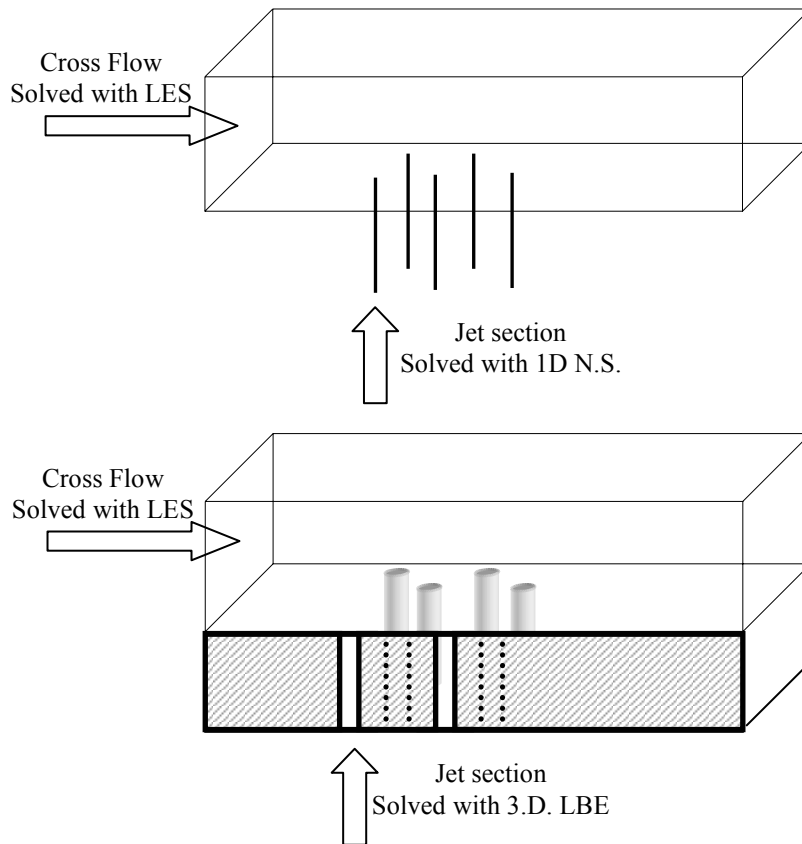


Figure 11. Schematic of two possible approaches to simulate the multi-port injection strategy. (a) Application of locally 1-D Navier-Stokes solver within each port, (b) Application of fully 3D LBE-LES model within each port. In both cases, the flow in the channel will be simulated by the 3D LES solver.

## 5.5 LES Method for Near-Wall and Multi-Port Injection Modeling

A new approach for high Re flows that departs significantly from conventional LES methodology has been developed. In conventional LES, the spatially filtered equations are solved on a "resolved" grid with a subgrid model for the small-scale motion. Current subgrid models specify the grid scale as the characteristic length scale and differ primarily in the specification of the velocity scale. The algebraic eddy viscosity subgrid model (Smagorinsky, 1963) and the one-equation model for the subgrid kinetic energy (Schumann, 1975) are two popular models. Dynamic variants of these models [10] have also been developed. In a recent study, a new two-level simulation (TLS) methodology has been developed that does not employ LES grid (or test) filtering, and in which both large- and small-scale fields are simulated simultaneously. The large-scale field is simulated on a conventional 3D grid while the small-scale motion evolves concurrently on a finer grid that is locally one-dimensional. The ability of this TLS approach in high-Re channel flows is evaluated so far and the results show the unique potential of this new approach. Further details are given elsewhere (Kemenov and Menon [36, 37]).

### 5.5.1 Key Features and Highlights of TLS studies

The following features distinguish TLS from LES:

1. TLS is not LES in the conventional sense since no grid or test filtering is carried out. Thus, TLS does not depend on the grid topology and hence, both structured and unstructured solvers can be used to resolve the large scales.
2. TLS simulates both the large-scale and the "un-resolved" small-scale fields simultaneously. The large scales evolve on a 3D grid, whereas the small-scales evolve on another (finer) grid that is embedded within the larger 3D grid.
3. The grid resolution for the small-scale field is fine enough to resolve the Kolmogorov scale. However, in order to reduce computational cost, the small-scale field is simulated on 3 1D orthogonal lines that are embedded within the 3D grid domain. This reduces the computational cost considerably.
4. Both large and small-scale fields are obtained by solving the 3D Navier-Stokes equations (without any explicit grid or test filtering). On the 3D grid, the flow equations contain terms that represent the contribution of the small scales. In the small-scale domain, a truncated 1D form of the Navier-Stokes equations is solved along the three 1D lines. These equations also contain terms that represent the effect of the resolved 3D field projected onto to the 1D lines. Thus, both large- and small-scale fields are fully coupled and evolve together.

### 5.5.2 Key Advantages of TLS over LES

The following key points identify the unique advantages of the TLS over LES.

1. TLS approach is not restricted by the high-resolution near-wall requirement in LES since in TLS the near-wall region is well resolved. Thus, TLS has potential for application to very high Re flows.
2. TLS is a small-scale simulation approach whereas conventional LES employs ad hoc subgrid models to represent the unresolved motion on the resolved field. As a consequence, all LES subgrid models have adjustable constants. Note that, the dynamic models which computes the constants using test filtering, assumes scale

- similarity between the resolved and unresolved scales. This approach will become highly questionable or even unstable when very high Re flows have to be simulated using relatively coarse grid.
3. Since the small-scales are simulated, there is additional information on how the small-scale fields evolve in the flow. Such information is non-existent in LES.
  4. The reduction of the small-scale domain into 3 1D lines reduces the form of the equations. In the TLS approach, the applicability and the validity of the local 1D approach depends upon the existence of a well-resolved inertial range. Thus, the TLS formulation becomes more accurate as the Reynolds number increases for given 3D grid resolution whereas conventional LES does not.
  5. Although TLS is computationally expensive it is highly parallel and is considerably cheaper than LES with DNS-level near-wall resolution.

### 5.5.3 TLS studies of 3D Channel Flow

The TLS approach has been used to study relatively high  $Re = 560$  3D channel flow. We chose this case since DNS data is available for direct comparison. The resolution used for DNS was relatively very high ( $384 \times 384 \times 384$ ) where as the TLS studies were conducted using  $32 \times 32 \times 32$  3D grid with 512 1D grid points within each 1D line. The results are summarized below. However, some key observations to note are that (a) the TLS approach allows the 3D grid size to be increased so that the near-wall region is no longer the constraint for the time-step, (b) the large and small-scale flow fields evolve in a consistent manner with the higher frequency scales of motion well resolved in the 1D grid, and (c) although some fine-tuning is needed, the results so far suggest that the TLS approach is a viable method for high Re flows without resorting to very high 3D grid resolution as in classical LES.

We present some preliminary results from a simulation of a relatively high Re channel flow for a  $Re = 590$ . The DNS study of this field was carried out earlier by Moser et al. [19] using a  $384 \times 257 \times 384$  grid. Here, we attempt to recover the flow field properties (mean and rms velocity fields) using a  $32 \times 32 \times 32$  large-scale grid and using 512 points along each 1D lines. Figures 12a and 12b show respectively, the instantaneous total streamwise velocity and the small-scale streamwise velocity in the wall normal direction. As expected, fine scale fluctuations are captured on the 1D line. Figures 13 and 14 show the comparison of the DNS results (solid lines) with the TLS predictions. Although there are some disagreements between the two results, it is clear that TLS approach is able to capture the essential features of the flow field even with a very coarse large-scale grid. Note that the peak in the velocity fluctuation occurs inside the first cell in the large-scale grid and is resolved by the 1D line. Further studies are still needed to refine this approach and also to evaluate its capability over wide range of high-Re flows. Additional research is still needed to determine this method's applicability to highly compressible flows and also for flows with multi-port injection. However, the base features of this approach are such that it can (at least theoretically) deal with complex flows. In any case, the TLS approach as implemented within the injection port holes will have to be modified for compatibility with the LES solver for the rest of the flow. This is an area of study at this time.

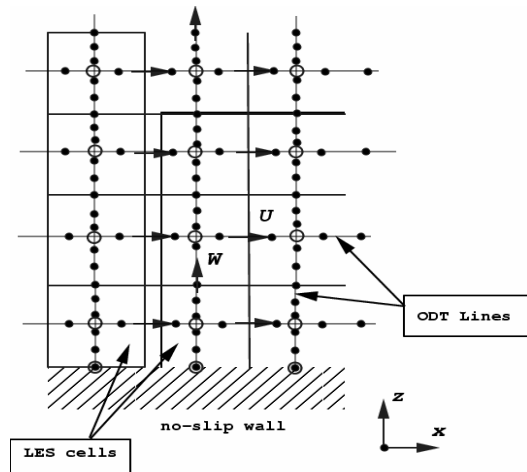


Figure 12. The two-level grid system. The resolved grid is 3D whereas the small-scale grid is 1D lines in each coordinate direction

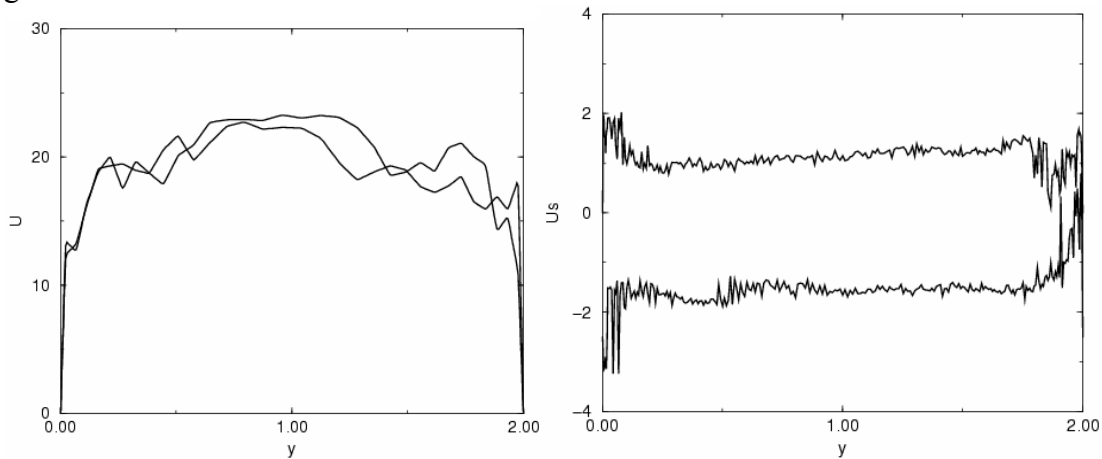


Figure 13. Two instantaneous snapshots of the flow field. (a) The total velocity field on the resolved grid, and (b) The small-scale field along wall-normal 1D lines (vertically shifted for visualization).

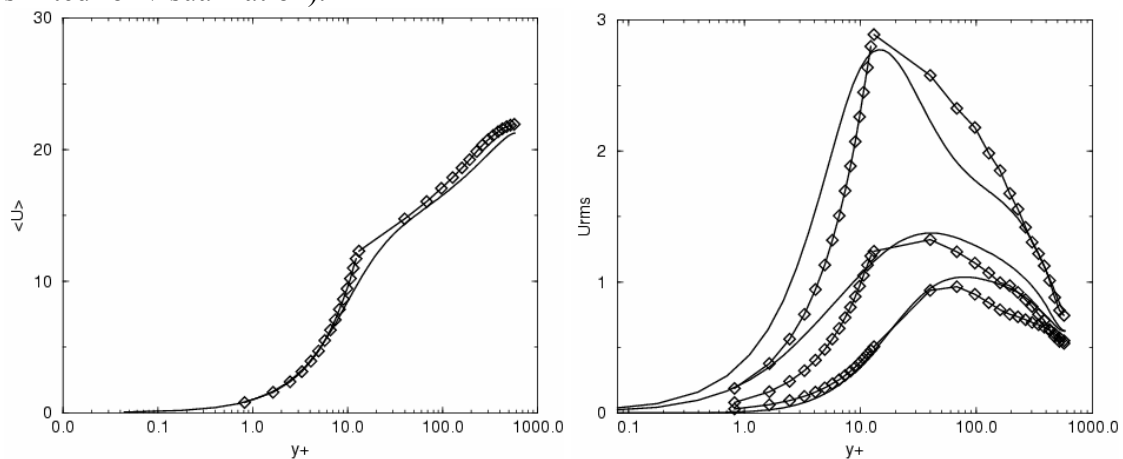


Figure 14. (a) The mean velocity profile in wall units. Line: DNS, Symbols: TLS, (b) The turbulent fluctuating velocities in descending order: streamwise, spanwise and wall normal components.

## 6. Conclusions and Future Plans

This report summarizes the progress made in the first 8 to 9 months of this research. As reported above, substantial progress has been made in all the proposed tasks. The LBE methodology for LES of microblowing has been validated using a jet-in-crossflow test configuration. In this study, the flow in the intake is also simulated to allow the interaction to occur naturally. As shown above, the LBELES approach is capable of capturing not only the flow features associated with this flow, such as hairpin vortices and recirculation behind the jet, but also is able to show better agreement with experiments when compared to previous RANS predictions. The LBELES is shown to be computationally very efficient and therefore, a viable method for simulating the injection process. This LBELES methodology will be further developed for the present application in the next phase of this research.

Another study has focused on validating the LES method for the flow in the experimental test channel. Preliminary validation for a low Reynolds number channel flow is shown for which there is DNS data for comparison. Comparison shows that LES method is able to capture the flow physics quite well.

Finally, two strategies have been developed to simulate multi-hole injection process as in the experiment. In order to allow natural interaction between the injected fluid and the primary stream the flow intake for all the holes have to be simulated. The LBE method is computationally efficient but is still 3D in nature and therefore, there may be some computational penalty in the long run. In order to study a large number of holes, a new 1D subgrid model has been developed that will simulate a reduced form of the Navier-Stokes equation in these holes. Preliminary validation for channel flow under another (ONR) project has shown the potential of this model for such simulations.

Future studies in the next quarter of the first year and in the subsequent second year will focus on the multi-port injection study of the experimental test case for Mach 0.4. Comparison with experimental data will be carried out. The goal of this phase will be to investigate how the near field flow in the boundary layer is being modified during this injection process. Additional simulations will be carried out in investigate if a combination of blowing and suction can be used to manipulate the over drag of the flow over the flat plate. Finally, a extension of this approach to even high Mach numbers: 0.8 to 1.9 will be developed during this second year.

## References

- [1] Hwang, D.P., "A Proof of Concept Experiment For Reducing Skin Friction By Using A Micro-Blowing Technique", AIAA-97-0546 (NASA TM-107315), 1997.
- [2] Hwang, D.P. and Biesiadny, T.J. (1997), "Experimental evaluation of the penalty associated with micro-blowing for reducing skin friction," NASA TM-113174.
- [3] Hwang, D.P. (1998), "Skin friction reduction by a microblowing technique," *AIAA J.*, Vol. 36, pp. 480-481.
- [4] Tillman, T.G. and Hwang, D.P. (1999), "Drag reduction on a Large-Scale Nacelle Using a Micro-Blowing Technique," AIAA Paper No. 99-0130.
- [5] Welch, G.E., Larosiliere, L.M., Hwang, D.P. and Wood, J.R. (2001) "Effectiveness of Micro-blowing technique in adverse pressure gradients," AIAA Paper No. 2001-1012.

- [6] Lin, Y.-L., Chyu, M.K., Shih, T.I-P., Willis, B.P., and Hwang, D.P. (1998), "Skin Friction Reduction through Micro-Blowing," AIAA Paper No. 98-0359, 36<sup>th</sup> Aerospace Sciences Meeting, Reno, NV.
- [7] Menon, S. (1999) "Computational Modeling of MEMS-based Micro-jets to Control Supersonic Boundary Layers," Computational Combustion Laboratory Technical Report CCL-99-002, Georgia Tech., April 1999.
- [8] Cammarato, J. and Menon, S. (1999) "Achieving aerodynamic stability through active boundary layer control utilizing MEMS," STTR Phase I final Report submitted by M. Technologies, Inc. to AFRL/MNAV, Eglin AFB, Florida, Contract No. F08630-98-C-0073.
- [9] Menon, S., Yeung, P.-K. and Kim, W.-W. (1996), "The Effect of Subgrid Models on the Computed Inter-scale Energy Transfer in Isotropic Turbulence," Computer and Fluids, Vol. 25, pp. 165-186.
- [10] Kim, W.-W. and Menon, S. (1999), "A New Incompressible Solver for Large-Eddy Simulations," International Journal of Numerical Methods in Fluids, Vol. 31, pp. 983-1017, 1999.
- [11] Kim, W-W. and Menon, S. (2000), "Numerical Modeling of Turbulent Premixed Flames in the Thin-Reaction-Zones Regime," Combustion Science and Technology, Vol. 160, pp. 113-150.
- [12] Kim, W.-W., Menon, S. and Mongia, H. (1999), "Numerical Simulations of Reacting Flows in a Gas Turbine Combustor," Combustion Science and Technology, Vol. 143, pp. 25-62, 1999.
- [13] Menon, S., Wang, H. and Kim, W.-W. (1999), "Lattice-Boltzmann Simulations of Micro-jet Controlled Fuel Injector Flow Fields," AIAA Paper 99-2118, 35<sup>th</sup> AIAA/ASME/SAE/ASEE Joint Propulsion Conference.
- [14] Menon, S. (1999), "Lattice-Boltzmann Simulations of Fuel Air Mixing, Controlled by Synthetic Micro-jets," Computational Combustion Laboratory Technical Report CCL-99-001, Georgia Tech., April.
- [15] Menon, S. (2000), "Fuel-Air Mixing Enhancement Using Synthetic Microjets," Computational Combustion Laboratory Technical Report CCL-00-002, Georgia Tech., March, 2000.
- [16] Menon, S. and Wang, H. (2001), "Fuel-Air Mixing using Embedded Synthetic Jets," AIAA Journal, Vol. 39, No. 12.
- [17] Smith, B.L. and Glezer, A. (1995) "Jet Vectoring by synthetic jet actuators," Bull. Am. Phys., Volume 40.
- [18] Fernando, E., and Menon, S. (1993), "Mixing Enhancement in Compressible Mixing Layers: An Experimental Study," AIAA Journal, Vol. 31, pp. 278-285, 1993.
- [19] Moser, R., Kim, J., and Mansour, N. (1999). Direct numerical simulation of turbulent channel flow up to  $Re = 590$ , J. of Fluid Mechanics, 11:943-945.
- [20] Nelson, C. and Menon, S. (1998), "Unsteady Simulations of Compressible Spatial Mixing Layers," AIAA Paper No. 98-0786, 36<sup>th</sup> Aerospace Sciences Meeting and Exhibit, Reno, NV, January 12-15, 1998.
- [21] Chen, H., S. Chen, and W.H. Matthaeus (1992) "Recovery of the Navier-Stokes equations using a lattice-gas Boltzmann method," Physical Review A, 45:5339-5342, 1992.

- [22] Qian, Y.H., D. d'Humieres and P. Lallemand (1992), "Lattice BGK models for the Navier-Stokes equation," Europhysics Letters, 17:479–484, 1992.
- [23] P.L. Bhatnager, E.P. Gross, and M. Krook (1954) "A model for collision process in gases. I. small amplitude process in charged and neutral one-component system," Physical Review A, 94:551–525, 1954.
- [24] Chen, S. and Doolen, G.D. (1998), "Lattice Boltzmann Method for Fluid Flows," Ann. Reviews of Fluid Mechanics, Vol. 30, pp. 329–367.
- [25] U. Frisch, B. Hasslacher, and Y. Pomeau. Lattice-gas automata for the navier-stokes equations. Physical Review Letters, 56:1505–1508, 1986.
- [26] Y.H. Qian, Succi S., and S.A. Orszag (1995) "Recent advances in Lattice Boltzmann computing," in Stauffer, D., Editor. Annual Reviews of Computational Physics III, pp. 195–242, 1995.
- [27] R. Mei, W. Shyy, D. Yu, and L.S. Luo. Lattice Boltzmann method for 3D flows with curved boundary. Journal of Computational Physics, 161:680–699, 2000.
- [28] Q. Zou and X. He (1997) "On pressure and velocity boundary conditions for the Lattice Boltzmann BGK model," Physics of Fluids, 9(6):1591–1598, 1997.
- [29] D.R. Noble, S. Chen, J.G. Georgiadis and R.O. Buckius (1995) "A consistent hydrodynamic boundary condition for the Lattice Boltzmann method," Physics of Fluids, 7(1):203–209, 1995.
- [30] R.S. Maier, R.S. Bernard, and D.W. Grunau (1996), "Boundary conditions for the Lattice Boltzmann method," Physics of Fluids, 8(7):1788–1801, 1996.
- [31] P. Ajresch, J. Zho, S. Ketler, M. Salcudean and I. Gartshore (1997), "Multiple jets in a crossflow: detailed measurements and numerical simulations," Journal of Turbomachinery, 119,330–342, 1997.
- [32] Lam, C.K.G., and Bremhorst, K.A. (1981), "Modified form of the  $k-\epsilon$  Model for predicting wall turbulence," Journal of Fluid Engineering, 103, 456–460.
- [33] Launder, B.E., and Tselepidakis, D.P. (1990), "Contribution to the second-moment modeling of sub-layer turbulent transport," Near-Wall Turbulence, Hemisphere, 818–833.
- [34] Chen, H.–C. (1995), "Submarine Flows Studied by second Moment closure," Journal of Engineering Mechanics, 121, 10, 1136–1146.
- [35] Yuan, Lester and Street, Robert and Ferziger, Joel (1999), "Large-eddy simulations of a round jet in crossflow," Journal of Fluid Mechanics, 379, 71–104.
- [36] Kemenov, K. and Menon, S. (2002), "TLS: A New Two-Level Simulation Methodology for High-Re LES," AIAA Paper 2002–0287.
- [37] Kemenov, K. and Menon, S. (2002), "A Two-Level Simulation Methodology for LES of High Reynolds Number Flows," in Advances in Turbulence IX, Castro et al. (Eds), pp. 203–206, CIMNE Press, Barcelona, Spain.
- [38] Menon, S. (2001), "Coupled Large-Eddy and Lattice Boltzmann Simulation of Synthetic Jet Enhanced Fuel Injector," Computational Combustion Laboratory Technical Report CCL–01–002, Georgia Tech, March 2001.

# REPORT DOCUMENTATION PAGE

*Form Approved*  
*OMB No. 0704-0188*

Public reporting burden for this collection of information is estimated to average 1 hour per response, including the time for reviewing instructions, searching existing data sources, gathering and maintaining the data needed, and completing and reviewing the collection of information. Send comments regarding this burden estimate or any other aspect of this collection of information, including suggestions for reducing this burden, to Washington Headquarters Services, Directorate for Information Operations and Reports, 1215 Jefferson Davis Highway, Suite 1204, Arlington, VA 22202-4302, and to the Office of Management and Budget, Paperwork Reduction Project (0704-0188), Washington, DC 20503.

<b>1. AGENCY USE ONLY</b> ( <i>Leave blank</i> )		<b>2. REPORT DATE</b> March 2003	<b>3. REPORT TYPE AND DATES COVERED</b> Annual Contractor Report—Jan. 2002–Sept. 2002	
<b>4. TITLE AND SUBTITLE</b> Large-Eddy/Lattice Boltzmann Simulations of Micro-Blowing Strategies for Subsonic and Supersonic Drag Control			<b>5. FUNDING NUMBERS</b>  WU-708-87-23-00 NAG3-2653	
<b>6. AUTHOR(S)</b>  Suresh Menon				
<b>7. PERFORMING ORGANIZATION NAME(S) AND ADDRESS(ES)</b> Computational Combustion Laboratory School of Aerospace Engineering Georgia Institute of Technology Atlanta, Georgia 30332-0150			<b>8. PERFORMING ORGANIZATION REPORT NUMBER</b>  E-13799	
<b>9. SPONSORING/MONITORING AGENCY NAME(S) AND ADDRESS(ES)</b>  National Aeronautics and Space Administration Washington, DC 20546-0001			<b>10. SPONSORING/MONITORING AGENCY REPORT NUMBER</b>  NASA CR—2003-212196	
<b>11. SUPPLEMENTARY NOTES</b>  Project Manager, Danny P. Hwang, Turbomachinery and Propulsion Systems Division, NASA Glenn Research Center, organization code 5850, 216-433-2187.				
<b>12a. DISTRIBUTION/AVAILABILITY STATEMENT</b>  Unclassified - Unlimited Subject Category: 02 Available electronically at <a href="http://gltrs.grc.nasa.gov">http://gltrs.grc.nasa.gov</a> This publication is available from the NASA Center for AeroSpace Information, 301-621-0390.			<b>12b. DISTRIBUTION CODE</b>	
<b>13. ABSTRACT</b> ( <i>Maximum 200 words</i> )  This report summarizes the progress made in the first 8 to 9 months of this research. The LBE methodology for LES of microblowing has been validated using a jet-in-crossflow test configuration. In this study, the flow intake is also simulated to allow the interaction to occur naturally. The LBELES approach is capable of capturing not only the flow features associated with the flow, such as hairpin vortices and recirculation behind the jet, but also is able to show better agreement with experiments when compared to previous RANS predictions. The LBELES is shown to be computationally very efficient and therefore, a viable method for simulating the injection process. Two strategies have been developed to simulate multi-hole injection process as in the experiment. In order to allow natural interaction between the injected fluid and the primary stream, the flow intakes for all the holes have to be simulated. The LBE method is computationally efficient but is still 3D in nature and therefore, there may be some computational penalty. In order to study a large number of holes, a new 1D subgrid model has been developed that will simulate a reduced form of the Navier-Stokes equation in these holes.				
<b>14. SUBJECT TERMS</b>  Micro-blowing technique; Drag control; Large-Eddy/Lattice Boltzmann Simulations			<b>15. NUMBER OF PAGES</b> 30	
			<b>16. PRICE CODE</b>	
<b>17. SECURITY CLASSIFICATION OF REPORT</b> Unclassified	<b>18. SECURITY CLASSIFICATION OF THIS PAGE</b> Unclassified	<b>19. SECURITY CLASSIFICATION OF ABSTRACT</b> Unclassified	<b>20. LIMITATION OF ABSTRACT</b>	